MOLECULAR AND CELLULAR BIOLOGY, Dec. 2006, p. 8928–8941 Vol. 26, No. 23
0270-7306/06/$08.00+0 doi:10.1128/MCB.00228-06

APPL1 Associates with TrkA and GIPC1 and Is Required for Nerve Growth Factor-Mediated Signal Transduction▽

Dan C. Lin,[1] Celia Quevedo,[1] Natalie E. Brewer,[2] Alex Bell,[3] Joseph R. Testa,[4] Mark L. Grimes,[5] Freda D. Miller,[1,6] and David R. Kaplan[1,6]*

Cancer Research Program and Developmental Biology Program, Hospital for Sick Children, Toronto M5G 1X8, Ontario, Canada[1]; Department of Neurology and Neurosurgery, McGill University, Montreal H3A 2B4, Quebec, Canada[2]; Department of Anatomy and Cell Biology, McGill University, Montreal H3A 2B2, Quebec, Canada[3]; Fox Chase Cancer Center, 333 Cottman Avenue, Philadelphia, Pennsylvania 19111[4]; Division of Biological Sciences, University of Montana, Missoula, Montana 59812-4824[5]; and Department of Medical Genetics and Microbiology, University of Toronto, Toronto M5S 1A8, Ontario, Canada[6]

Received 7 February 2006/Returned for modification 28 March 2006/Accepted 3 September 2006

The neurotrophin receptor TrkA plays critical roles in the nervous system by recruiting signaling molecules that activate pathways required for the growth and survival of neurons. Here, we report APPL1 as a TrkA-associated protein. APPL1 and TrkA coimmunoprecipitated in sympathetic neurons. We have identified two routes through which this association can occur. APPL1 was isolated as a binding partner for the TrkA-interacting protein GIPC1 from rat brain lysate by mass spectrometry. The PDZ domain of GIPC1 directly engaged the C-terminal sequence of APPL1. This interaction provides a means through which APPL1 may be recruited to TrkA. In addition, the APPL1 PTB domain bound to TrkA, indicating that APPL1 may associate with TrkA independently of GIPC1. Isolation of endosomal fractions by high-resolution centrifugation determined that APPL1, GIPC1, and phosphorylated TrkA are enriched in the same fractions. Reduction of APPL1 or GIPC1 protein levels suppressed nerve growth factor (NGF)-dependent MEK, extracellular signal-regulated kinase, and Akt activation and neurite outgrowth in PC12 cells. Together, these results indicate that GIPC1 and APPL1 play a role in TrkA function and suggest that a population of endosomes bearing a complex of APPL1, GIPC1, and activated TrkA may transmit NGF signals.

The TrkA receptor tyrosine kinase is essential for the development and function of the vertebrate nervous system. As a receptor for the prototypic neurotrophin nerve growth factor (NGF), TrkA propagates NGF-induced signaling cascades required for the survival, differentiation, growth, and function of neurons. Within the peripheral nervous system, NGF and other members of the neurotrophin family are target derived and secreted in limiting amounts to ensure appropriate innervation by supporting the survival of only those neurons that have made the correct connections (21, 22). In particular, once axons have reached their targets, NGF binds to TrkA on axonal terminals. The subsequent activation of TrkA stimulates the activities of the mitogen-activated protein kinase (MAPK), phosphatidylinositol (PI) 3-kinase/Akt, and phospholipase C (PLC)-γ pathways (19, 28). A number of these NGF-mediated signals are transmitted in a retrograde fashion from the terminal along the axon to the cell body and, ultimately, to the nucleus to elicit transcriptional responses. Those neurons that receive sufficient retrograde survival and growth signals survive and innervate their targets, while those that do not are eliminated by apoptosis.

Accumulating evidence indicates that one means by which the retrograde signal is transduced is in an endosome (2, 9, 15) that is generated by internalization of the TrkA receptor through both clathrin-dependent (14) and clathrin-independent (30, 35) mechanisms. Within the endosome, NGF, activated TrkA, and components of TrkA signaling pathways are found together and create a discrete signaling unit that is transported along the axon to the cell body (4, 6, 7, 10, 11, 14, 18, 33, 37, 40). Thus, TrkA functions not only as a receptor at the plasma membrane but also as a signaling entity within the cell. In this manner, the signaling function of TrkA is also tied to its trafficking.

While a number of interacting partners for TrkA have been identified, relatively few proteins have been shown to link TrkA signaling to its trafficking. One TrkA-associated protein that may fulfill this function is the PDZ domain-containing protein GIPC1. GIPC1 is constitutively associated with TrkA and TrkB through direct binding to the juxtamembrane region of the receptor. Overexpression of GIPC1 in PC12 cells decreases NGF-induced extracellular signal-regulated kinase 1 (ERK1) and ERK2 activation, implicating GIPC1 in TrkA signaling (24). Several lines of evidence suggest that GIPC1 may be involved in endocytosis and early trafficking events. GIPC1 localizes to clathrin-coated pits and peripheral endosomes in the rat kidney and in ARPE-19 retinal pigmented epithelial cells (1, 23). A potential function for GIPC1 in vesicular transport is suggested by its association with motor proteins KIF-1B and myosin VI (5). In NGF-treated PC12 cells, phosphorylated TrkA (pTrkA) and GIPC1 colocalize in endocytic structures (24). GIPC1 has been postulated to act as a scaffolding protein and, as such, could act to recruit other proteins to TrkA, nucleating multiprotein complexes important for TrkA signaling and trafficking.

One family of molecules that has been shown to link signal-

* Corresponding author. Mailing address: Cancer Research Program, Hospital for Sick Children, 555 University Ave., Toronto M5G 1X8, Ontario, Canada. Phone: (416) 813-7654, ext. 1433. Fax: (416) 813-2212. E-mail: dkaplan@sickkids.ca.

▽ Published ahead of print on 25 September 2006.

ing and trafficking downstream of receptor tyrosine kinases are the APPL proteins. APPL1 and APPL2 act to couple receptor trafficking to epidermal growth factor (EGF) signaling via an endocytic compartment in HeLa cells (26). APPL associates with the small-molecular-weight GTPase Rab5, a key regulator of transport from the plasma membrane to the early endosome (32, 41). Upon EGF treatment and subsequent hydrolysis of GTP-Rab5, APPL1 and APPL2 are released from the plasma membrane and translocate to the nucleus, where they associate with components of the nucleosome remodeling and histone deacetylation machinery. The endosomal signaling pathway mediated by APPL1 and APPL2 links signaling events at the plasma membrane with chromatin remodeling in the nucleus and is essential for cell proliferation.

In the present study, we have identified APPL1 as a new TrkA-interacting protein. APPL1 associates with TrkA through two different means: indirectly via GIPC1 through a PDZ domain-mediated interaction and directly through the APPL1 phosphotyrosine binding (PTB) domain. Cell fractionation studies demonstrate that APPL1, GIPC1, and pTrkA are present in the same endosomal fractions. Last, we demonstrate roles for APPL1 and GIPC1 in TrkA function by determining that both proteins are required for NGF-induced MEK, ERK1/2, and Akt activation and neurite outgrowth. This study extends the function of APPL1 to neurotrophin receptor signaling and is consistent with a potential role for APPL1 in the signaling endosome downstream of NGF.

MATERIALS AND METHODS

Constructs, mutagenesis, fusion proteins, and antibodies. The Flag-GIPC1 pcDNA3 (Invitrogen) template was kindly provided by Moses Chao. For glutathione-*S*-transferase (GST) fusion constructs, cDNA sequences of rat GIPC1 (full length, residues 1 to 333; N terminus, residues 1 to 108; N terminus plus PDZ, residues 1 to 216; PDZ, residues 109 to 216; C terminus, residues 216 to 333) were cloned into the pGEX2 vector (GE Healthcare). Constructs encoding APPL1 fusion proteins were created by amplifying regions of the human APPL1 cDNA corresponding to the full length (residues 1 to 709), the Bin-amphiphysin-Rvs (BAR) domain (residues 1 to 269), the pleckstrin homology (PH) domain (residues 263 to 480), the PTB domain (residues 472 to 655), and the PTB domain plus the C terminus (residues 472 to 709) and subcloning in frame into pFLAG CMV2 (where CMV is cytomegalovirus), pEYFP (where EYFP is enhanced yellow fluorescent protein) (Clontech), pGEX4T3 (GE Healthcare), or pPRO EX HTc (Invitrogen). Constructs encoding TrkA fusion proteins were generated by amplifying segments of human TrkA cDNA corresponding to the juxtamembrane region (residues 434 to 510), the kinase domain (residues 502 to 660), and the C-terminal region (residues 660 to 790) and subcloning in frame into pPRO EX HTc. Mutations in the GIPC1 and APPL1 cDNAs were generated using a QuikChange site-directed mutagenesis kit (Stratagene). All fusion constructs and mutations were confirmed by sequencing. GST and His fusion constructs were used to transform an *Escherichia coli* BL21 strain, and the recombinant fusion proteins were purified using standard procedures.

Rabbit polyclonal antibodies were raised separately against GST fusions of full-length GIPC1 and APPL1 PTB plus the C terminus. Rabbits were immunized and boosted at 6-week intervals by use of standard methods. Antibodies against APPL1 were affinity purified by applying raw sera to a GST-Sepharose column to deplete anti-GST antibodies, followed by enrichment through a GST-APPL1 PTB plus C terminus Sepharose column. Rabbit anti-TrkA RTA was a gift from L. Reichardt (University of California, San Francisco, CA). The rabbit anti-pan-Trk antibody has been described previously (12). Other antibodies used were mouse anti-Flag M2 (Sigma); mouse anti-tetra-His (QIAGEN); mouse antiphosphotyrosine (4G10; Upstate Biotechnology); rabbit anti-phospho-(Tyr490) TrkA, rabbit anti-p(Ser-217/Ser-221) MEK, rabbit anti-MEK, rabbit anti-phospho(Tyr317) Shc, rabbit anti-Akt, and rabbit anti-phospho(Ser-473) Akt (Cell Signaling); rabbit anti-phospho(Thr-183/Tyr-185) ERK (Promega); mouse anti-green fluorescent protein (anti-GFP) (Molecular Probes); rabbit anti-ShcA (Upstate Biotechnology); mouse anti-Trk (Zymed); and rabbit anti-ERK1 (Santa Cruz).

Mass spectrometry and peptide analysis. Adult rat brains were homogenized in 10 mM HEPES, pH 7.4, supplemented with Mini Complete protease inhibitor cocktail (Roche) and 1.5 mM sodium vanadate. Triton X-100 was added to 1%, and the homogenate was incubated at 4°C for 20 min. The soluble fraction was isolated through centrifugation at 10,000 × *g* for 30 min at 4°C. Lysates were incubated with 5 μg GST-GIPC1 fusion protein for 2 h at 4°C. Beads were subsequently washed three times in lysis buffer containing 1% Triton X-100. GST-GIPC1-associated proteins were separated by sodium dodecyl sulfate-polyacrylamide gel electrophoresis (SDS-PAGE) and stained with Coomassie brilliant blue. Bands were excised, reduced, alkylated, and in-gel trypsin digested as described previously (36a). The resulting peptide extracts were analyzed by employing a nanoscale liquid chromatography quadrupole time of flight mass spectrometer. The resulting MS were analyzed by Mascot software (cluster version 1.9.03).

Cell culture, primary sympathetic neuron cultures, transfection, and growth factors. COS7 cells were cultured in Dulbecco's modified Eagle medium (DMEM) supplemented with 10% fetal bovine serum, 120 μg/ml penicillin, 200 μg/ml streptomycin sulfate, and 600 μg/ml glutamine. PC12 (clone 6-24) cells which stably overexpress TrkA (12) were maintained in DMEM containing 10% horse serum, 5% bovine calf serum, 120 μg/ml penicillin, 200 μg/ml streptomycin sulfate, 600 μg/ml glutamine, and 200 μg/ml Geneticin (Invitrogen). Mass cultures of sympathetic neurons derived from the superior cervical ganglia (SCG) of postnatal day 1 Sprague-Dawley rats were prepared and cultured as described previously (34). NGF was withdrawn from sympathetic neuron cultures by performing three 1.5-h washes in Ultraculture medium (Cambrex) without NGF. For neurotrophin inductions, NGF at a final concentration of 50 ng/ml was added to the media for 10 min prior to cell lysis. For experiments performed in the presence of Trk inhibitor, 200 nM K252a (Calbiochem) was added to sympathetic neuron cultures prior to NGF treatment. Transient transfections were performed using Lipofectamine 2000 and Opti-MEM as outlined by the manufacturer (Invitrogen). For transient transfection of SCG cultures, primary cultures were transfected at the time of plating in Ultraculture medium containing 120 μg/ml penicillin, 200 μg/ml streptomycin sulfate, 600 μg/ml glutamine, 50 ng/ml nerve growth factor, 3% rat serum (Wisent, Inc.), 0.7% cytosine β-arabinofuranoside (Sigma), and 50 mM potassium chloride. NGF was obtained from Cedarlane Labs, Ltd.

Recombinant adenovirus and viral infection. Replication-defective recombinant adenovirus encoding wild-type human TrkAI containing a Flag tag epitope in the extracellular domain has been described previously (20). Viral infections of sympathetic neurons were performed as described previously (25, 36). Cells were infected with 100 multiplicities of infection of virus overnight and assayed 48 h after infection.

Immunoprecipitation and Western blot analysis. Cells were rinsed twice in ice-cold phosphate-buffered saline (PBS) and lysed in PLC lysis buffer supplemented with 10 μg/ml aprotinin, 10 μg/ml leupeptin, 1 mM sodium vanadate, and 1 mM phenylmethylsulfonyl fluoride (PMSF) (13). Immunoprecipitations were performed for 2 h at 4°C with antibodies at a concentration of 1 μg/ml and either protein A or goat anti-mouse Sepharose. GST mixing experiments were carried out by incubating lysate with 5 μg of fusion protein immobilized on glutathione-Sepharose for 2 h at 4°C. To measure direct binding of GIPC1 to APPL1, 1 μg of bacterially produced, purified His-tagged fragments of APPL1 was incubated with 5 μg of the purified recombinant GST-GIPC1 fusion proteins bound to glutathione-Sepharose. Experiments to assay direct binding of APPL1 to TrkA were performed by incubating 1 μg of bacterially produced, purified His-tagged fragments of TrkA with 5 μg of the purified recombinant GST-APPL1 fusion proteins bound to glutathione-Sepharose. For the peptide mixing experiments, 1.25 nmol of biotinylated TrkA or pTrkA peptide or, as a negative control, 1.25 nmol of biotin was incubated with 15 μl of high-performance streptavidin Sepharose (GE Healthcare) for 1 h at 4°C. Beads were washed twice in PLC buffer to remove unbound peptide and then incubated with 2 mg of PC12 (6-24) lysate for 2 h at 4°C. The TrkA Shc-binding site peptide of sequence biotin-Aca-AAVALLPAVLLALLAPHIIENPQYFSD and the related phosphopeptide biotin-Aca-AAVALLPAVLLALLAPHIIENPQpYFSD were a kind gift from Jerry Gish. In both immunoprecipitation and mixing experiments, beads were washed three times in HNTG buffer containing 10 μg/ml aprotinin, 10 μg/ml leupeptin, 1 mM sodium vanadate, and 1 mM PMSF (13). Proteins were separated by SDS-PAGE, transferred to nitrocellulose membrane, and immunoblotted with the appropriate antibody. Blots were developed by enhanced chemiluminescence (GE Healthcare). For Western blot analysis of endosomal fractions, luminescence was measured using a cooled charge-coupled-device camera with a Fuji LAS-3000 system and data were quantified with Fuji Image Gauge software.

Densitometric analyses of other immunoblots were performed on scanned films with Total Lab 1.0 software (GE Healthcare). Intensity values were normalized to measurements of the ERK1 and MEK loading controls.

Preparation of endosomal fractions. PC12 cells (10^9) grown on collagen-coated plates in RPMI 1640, 5% fetal calf serum, and 10% horse serum were harvested in ice-cold PBS. Cells were rinsed in PBS containing 1 mM EGTA and 1 mM EDTA, followed by one wash in PBS with 0.1% glucose and 0.1% bovine serum albumin (PGB). To ensure precise control of internalization time, cells were treated with 50 ng/ml NGF at 4°C in PGB for 1 h to allow binding to the receptor, washed in PGB to remove unbound ligand so as to avoid fluid-phase endocytosis, and warmed in PGB to 37°C for 10 min, followed by a temperature quench in ice water. Following washes in PBS containing 1 mM EGTA and 1 mM EDTA and then buffer B (cytoplasmic ionic composition of 38 mM each of the K^+ salts of aspartic acid, glutamic acid, and gluconic acid, 20 mM MOPS [morpholinepropanesulfonic acid], pH 7.1, at 37°C, 10 mM potassium bicarbonate, 0.5 mM magnesium carbonate, 1 mM EDTA, 1 mM EGTA), cells were resuspended in buffer B supplemented with 5 mM reduced glutathione, protease inhibitors (0.1 μg/ml aprotinin, chymostatin, leupeptin, and pepstatin A; 1 μg/ml 1,10-phenanthroline; 10 μg/ml bisbenzamide; and 1 mM PMSF), and phosphatase inhibitors (100 nM calyculin A and 1 mM sodium vanadate). Mechanical permeabilization of cells was performed by a single passage through a Balch homogenizer as described previously (10, 11).

Semi-intact cells and large membranes were removed from the permeabilized cell suspension by centrifugation at 1,000 × *g*. The resulting supernatant (S1) was layered over a 0 to 30% iodixanol velocity gradient and centrifuged at 133,000 × *g* for 1.5 h. Five fractions were collected from velocity gradients and further resolved by equilibrium gradient centrifugation: fractions were mixed with 60% iodixanol to a concentration of 32.5% or greater, overlaid with a continuous 0 to 30% iodixanol-buffer B plus glutathione gradient, and centrifuged to equilibrium (16 to 18 h). Twenty-four fractions were collected from each equilibrium gradient. To determine density, refractive indices were measured using an Abbe refractometer (Bausch and Lomb) and converted to density using the formula $\rho = RI \times 3.4319 - 3.5851$, where RI is refractive index. This formula was determined empirically by weighing known concentrations of iodixanol in buffer B.

siRNA preparation and transfection. Duplex small interfering RNAs (siRNAs) targeted against rat APPL1 (5′-CUCACCUGACUUCGAAACUTT and 5′-AGUUUCGAAGUCAGGUGAGTT) or against rat GIPC1 (5′-AGAGGU GGAAGUAUUCAAGTT and 5′-CUUGAAUACUUCCACCUCUTT) or of a nonspecific sequence (5′-UCUUGUCGAUCGGUGUUCUTT and 5′-AGAAC ACCGAUCGACAAGATT) were purchased from Dharmacon. For biochemical studies, PC12 (6-24) cells plated in 12-well tissue culture plates at a density of 16,000 cells per well were transfected 24 h later with 100 nM of siRNA oligonucleotides by use of Lipofectamine 2000. To evaluate NGF-induced ERK and Akt activation, cells were rinsed twice in DMEM at 3-h intervals to remove serum 42 h posttransfection. Forty-eight hours following transfection, 50 ng/ml NGF was added to the medium for 10 min and cell lysates were prepared for analysis. For neurite outgrowth assays, PC12 (6-24) cells plated on 30 μg/ml poly-L-lysine in 12-well tissue culture plates at a density of 16,000 cells per well were cotransfected with 1 μg pEGFP (where EGFP is enhanced green fluorescent protein) (Clontech) and 100 nM of siRNA oligonucleotides. Cells were treated with 50 ng/ml NGF in DMEM containing 0.5% horse serum 24 h posttransfection to allow neurite outgrowth. Following 48 h of NGF treatment, images were captured using a Retiga Exi digital camera (Q-imaging) on a Zeiss Axiovert 200 M inverted microscope equipped with fluorescence optics. For each condition, 24 images of random fields were taken at a ×20 magnification from two wells. Neurite lengths of GFP-positive cells were measured using Northern Eclipse software (Empix Imaging). The experiment was performed three times. From the three experiments, the total number of cells analyzed was 279 for APPL1 siRNA/pEGFP-cotransfected cells, 359 for GIPC1/pEGFP-cotransfected cells, and 563 for siRNA control/pEGFP-cotransfected cells. Statistical analyses were carried out using SAS software, version 8.02 (SAS Institute, Inc.). Tukey and Bonferroni tests were performed using the generalized linear model procedure. MTT (3-[4,5-dimethylthiazol-2-yl]-2,5-diphenyltetrazolium) assays were performed as previously described (36).

Immunofluorescence microscopy. Cells were rinsed briefly in PBS, fixed with 4% paraformaldehyde in PBS for 20 min, permeabilized with 0.1% Triton X-100 in PBS for 5 min, and placed in blocking solution (5% bovine serum albumin, 5% normal goat serum, and 0.01% Tween 20 in PBS) for 1 h at room temperature. Single- or double-label immunofluorescence staining procedures were employed to detect endogenous APPL1, endogenous TrkA, and exogenous Flag-GIPC1. Samples were incubated overnight at 4°C with primary antibodies at a concentration of 1 μg/ml in blocking solution. Alexa 488-conjugated anti-mouse, Alexa 488-conjugated anti-rabbit, Alexa 555-conjugated anti-mouse, and Alexa 555-conjugated anti-rabbit antibodies (Molecular Probes) were used to detect primary antibodies. Nuclei were visualized by staining with Hoechst reagent at a concentration of 0.5 μg/ml. Microscopy was carried out using a Zeiss Axiovert 200 M inverted microscope equipped with fluorescence optics. Confocal images were taken on a Zeiss LSM510 META laser scanning confocal microscope.

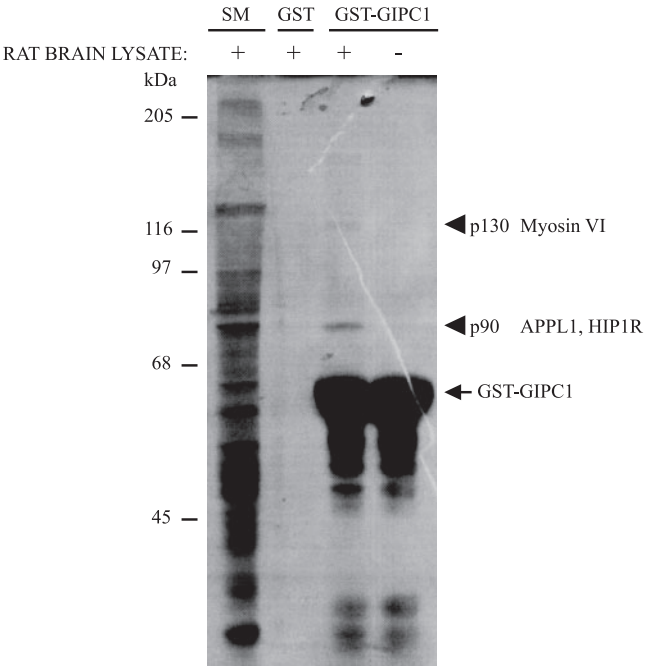

FIG. 1. Identification of APPL1 as a binding partner for GIPC1. Cellular proteins precipitated with a GST fusion of full-length GIPC1 were isolated from adult rat brain extracts. Interacting proteins were resolved by SDS-PAGE and detected by staining with Coomassie brilliant blue. Total cellular proteins representing the starting material (SM) are shown in the first lane. Addition of GST alone to lysate and incubation of GST-GIPC1 in the absence of lysate were included as negative controls. The GST-GIPC1 band is marked with an arrow. Bands specifically precipitated with GST-GIPC1 (marked with arrowheads) were excised from the gel and digested with trypsin. The resulting peptides were sequenced by mass spectrometry.

RESULTS

Identification of binding partners for GIPC1 by mass spectrometry. To identify potential interacting partners for GIPC1 within the nervous system, a GST fusion of full-length GIPC1 was incubated with adult rat brain lysate. Captured proteins were resolved by SDS-PAGE and visualized by Coomassie blue staining. This approach detected two bands, at 130 kDa and 90 kDa, that bound specifically to GST-GIPC1 but not to GST alone (Fig. 1). Analysis of the excised proteins by liquid chromatography quadrupole time of flight assisted laser desorption ionization mass spectrometry identified three proteins as putative binding partners for GIPC1.

Ten peptides were detected within the 130-kDa band which matched the sequence of the unconventional myosin myosin VI. The isolation of myosin VI, a known interacting partner for GIPC1 (5), confirmed the efficacy of the screen. The prominent band, migrating at a relative molecular mass of 90 kDa, yielded tryptic peptides homologous to sequences of two different proteins. Ten peptides were identified with sequence corresponding to Huntingtin interacting protein 1 related

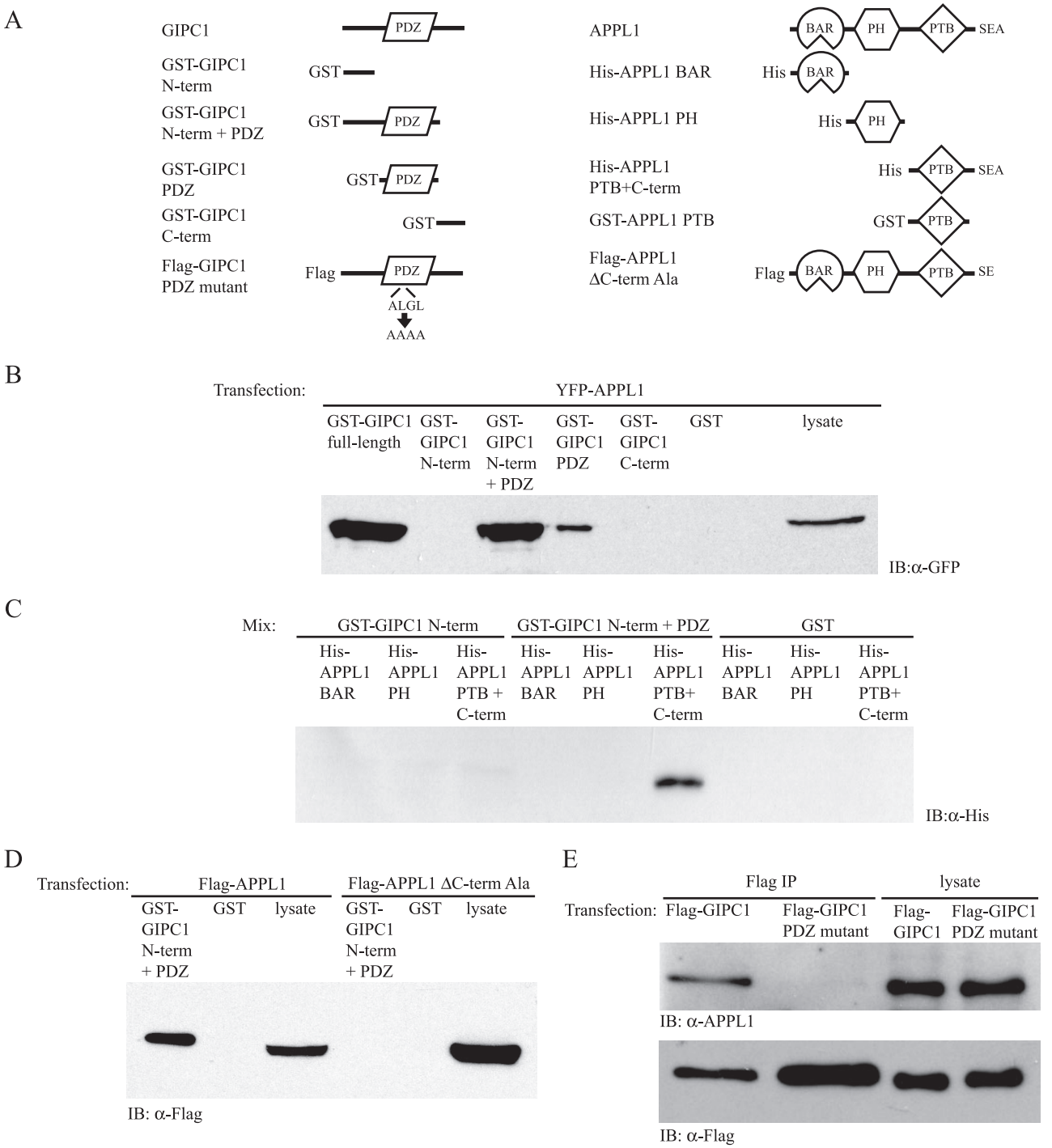

FIG. 2. The PDZ domain of GIPC1 binds directly to the C terminus of APPL1. (A) Schematic representations of the domain architecture of GIPC1 (left) and APPL1 (right). GST, Flag, and His epitope-tagged fusions of fragments and mutants of GIPC1 and APPL1 are shown. (B) GST fusions of full-length GIPC1 or fragments of GIPC1 containing the PDZ domain specifically precipitate YFP-APPL1 from lysates of transfected COS7 cells. Cell lysates were incubated with the GST fusion proteins as indicated, and the resulting complexes were analyzed by immunoblotting (IB) with anti-GFP antibody. (C) The PDZ domain of GIPC1 is necessary and sufficient for direct association with the C-terminal region (C-term) of APPL1. Purified fragments of APPL1 fused to a His epitope were incubated with purified, Sepharose-immobilized GST fusions of the GIPC1 N terminus (N-term), GIPC1 N terminus plus PDZ (N-term + PDZ), or GST alone. Anti-His antibody was used to detect His-APPL1 proteins by immunoblotting. (D) Removal of the C-terminal alanine residue of APPL1 (ΔC-term Ala) abrogates its association with GIPC1. COS7 cells were transiently transfected to express either wild-type Flag-APPL1 or Flag-APPL1 ΔC-term Ala. Cell lysates were incubated with GST fusion proteins as indicated and analyzed by immunoblotting with anti-Flag antibody. Lysates of transfected cells show expression levels of the wild-type and truncated proteins. (E) Mutation of the carboxylate-binding loop within the GIPC1 PDZ domain eliminates its interaction with APPL1. Flag-GIPC1 and the Flag-GIPC1 PDZ mutant were immunoprecipitated (IP) from transfected COS7 cells with anti-Flag antibody. Endogenous APPL1 associated with Flag-GIPC1 was detected with antibodies against APPL1 (top). Levels of Flag-GIPC1 proteins were determined using the anti-Flag antibody (bottom).

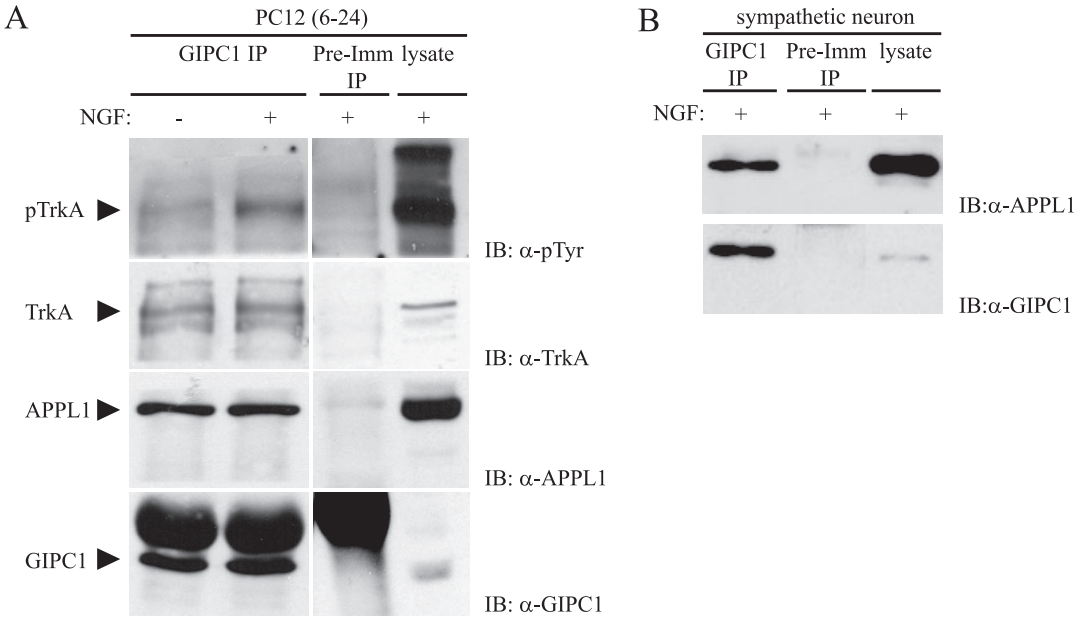

FIG. 3. GIPC1 and APPL1 associate in cells. (A) APPL1, TrkA, and pTrkA coprecipitate with GIPC1 in PC12 (6-24) cells. Endogenous GIPC1 was precipitated from lysates of cells treated with 50 ng/ml NGF for 10 min (+) or from untreated cells (−). The presence of endogenous APPL1, TrkA, and pTrkA in the precipitates was detected by immunoblotting (IB) with anti-APPL1, anti-TrkA, and antiphosphotyrosine antibodies, respectively. Immunoprecipitation with preimmune serum (Pre-Imm IP) was included as a negative control. TrkA, pTrkA, APPL1, and GIPC1 proteins are marked with arrowheads. The upper band in the anti-GIPC1 immunoblot is the immunoglobulin heavy chain. (B) APPL1 coprecipitates with GIPC1 in rat primary sympathetic neurons. Endogenous GIPC1 was precipitated from sympathetic neuron lysates treated with 50 ng/ml NGF for 10 min. Immunoblots were probed with the indicated antibodies.

(HIP1R) peptide, and 16 peptides were detected corresponding to APPL1. Consistent with the function of many of the GIPC1-interacting proteins identified to date, HIP1R is a component of clathrin-coated pits and vesicles, supporting a role for GIPC1 in endocytosis (8). APPL1 plays a key role in endosomal signaling that links events initiated by EGF at the plasma membrane to chromatin remodeling in the nucleus (26). Specialized endosomes containing TrkA have been shown to relay NGF-mediated survival and differentiation signals from the axon to the cell body. Therefore, we chose to investigate the interaction between APPL1 and GIPC1 in the context of TrkA function.

The PDZ domain of GIPC1 interacts directly with the C terminus of APPL1. In order to verify the interaction between GIPC1 and APPL1, a GST fusion of full-length GIPC1 was incubated with lysates of COS7 cells transfected to express YFP-APPL1. Recovery of the fusion protein and immunoblotting of bound proteins with anti-GFP antibody confirmed that GIPC1 bound specifically to APPL1 and not the GST control (Fig. 2B). The region of GIPC1 mediating the interaction was defined using portions of GIPC1 protein fused to GST (Fig. 2A). Fragments encompassing the N-terminal region and the PDZ domain of GIPC1 as well as the PDZ domain alone were observed to bind to APPL1, whereas no interaction was detected with the N-terminal or the C-terminal region of GIPC1 alone (Fig. 2B). These results indicate that the PDZ domain of GIPC1 is necessary and sufficient for APPL1 binding.

To test whether the interaction was direct and to map the binding site on APPL1, we incubated His-tagged fusions of fragments of APPL1 spanning the length of the protein (Fig. 2A) with purified GST fusions of GIPC1. A GST fusion protein of the N-terminal region and PDZ domain of GIPC1 associated directly with the C-terminal third of APPL1 (Fig. 2C). No binding of this GIPC1 fragment was detected with the N-terminal BAR domain or the central PH domain of APPL1. These results are indicative of a direct interaction between the PDZ domain of GIPC1 and the C-terminal sequence of APPL1.

To evaluate if these regions of APPL1 and GIPC1 were necessary for the proteins to interact, mutations in APPL1 and GIPC1 which we predicted would disrupt their association were generated. PDZ domains typically bind short sequences of 4 to 5 residues at the extreme carboxy terminus of their target protein. Mammalian APPL1 proteins possess a putative PDZ domain binding site (ESEA-CO_2H). Deletion of the C-terminal alanine residue of APPL1 effectively abrogated its binding to a GST fusion of the N-terminal region and PDZ domain of GIPC1, confirming that the very C-terminal residues of APPL1 constitute a binding site for the GIPC1 PDZ domain (Fig. 2D). In a complementary experiment, mutation of each of the residues comprising the carboxylate-binding loop of the GIPC1 PDZ domain to alanine eliminated its association with APPL1 (Fig. 2E). Taken together, these observations clearly demonstrate that GIPC1 and APPL1 associate directly via a canonical interaction between the PDZ domain of GIPC1 and the short carboxy-terminal sequence of APPL1.

APPL1 associates with GIPC1 in cells. GIPC1 has previously been reported to associate with TrkA in PC12 cells (24). The identification of APPL1 as an interacting partner for

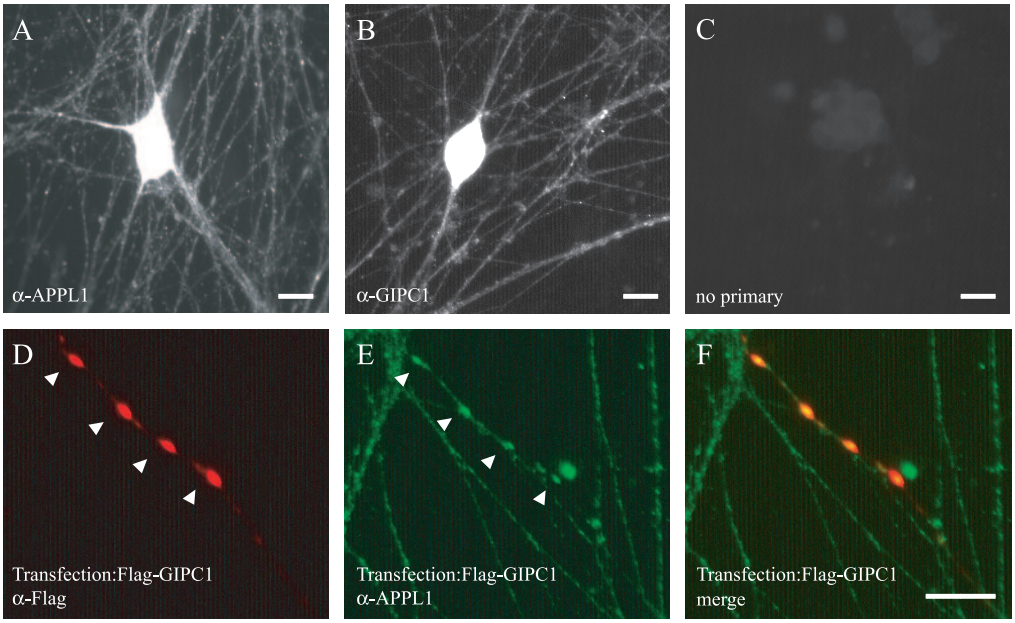

FIG. 4. APPL1 and GIPC1 share similar codistribution patterns in sympathetic neurons. Endogenous APPL1 (A) and GIPC1 (B) display punctate patterns of distribution in axons of sympathetic neurons cultured in medium containing NGF. Neurons from newborn rat SCG were immunostained with an antibody against APPL1 or GIPC1 as indicated. (C) As a negative control, primary antibody was omitted. (D) Anti-Flag staining (red) of an axon from a sympathetic neuron transiently transfected to express Flag-GIPC1. (E) Distribution of endogenous APPL1 (green) as determined by immunofluorescence staining with anti-APPL1 antibody. The same field is shown in panel D. Arrowheads mark examples of Flag-GIPC1 and endogenous APPL1 codistribution (D and E). (F) Merged image of panels D and E. Bar, 10 μm.

GIPC1 provides a possible link between APPL1 and TrkA. Therefore, we were interested in determining if APPL1 and GIPC1 associate in cells where TrkA function has been characterized extensively. PC12 cells and sympathetic neurons are prototypical models for examining the requirement of TrkA signaling for growth and survival. Since APPL1 expression has not been reported for these cell types, we assessed expression of APPL1 in PC12 (6-24) cells stably overexpressing TrkA and in cultured sympathetic neurons from postnatal day 1 rat SCG. Western blotting with an antibody generated against the PTB domain of APPL1 detected robust levels of APPL1 in both cell types (Fig. 3A and B). The subcellular localization of APPL1 and GIPC1 in sympathetic neurons was determined by immunofluorescence staining. Endogenous APPL1 (Fig. 4A) and endogenous GIPC1 (Fig. 4B) were present in a punctate pattern in axons. The specificity of the pattern was confirmed by staining in the absence of primary antibody as a negative control (Fig. 4C).

Having confirmed expression, we asked if endogenous APPL1 and GIPC1 form complexes in these cells. To evaluate whether APPL1 and GIPC1 exhibit a codistribution pattern, sympathetic neurons were transiently transfected to express Flag-GIPC1. Costaining with antibodies against the Flag epitope and against APPL1 revealed a punctate colocalization of Flag-GIPC1 and endogenous APPL1 in axons of transfected cells (Fig. 4D to F). Next, we performed coprecipitation experiments to determine if endogenous APPL1 and GIPC1 interact. Immunoprecipitation of GIPC1 coprecipitated APPL1 in both PC12 cells and sympathetic neurons (Fig. 3A and B). Precipitation with preimmune serum did not yield detectable APPL1, indicating that the interaction is specific. APPL1 was present at comparable levels in GIPC1 immunoprecipitates from untreated PC12 cells and from cells treated with 50 ng/ml NGF for 10 min (Fig. 3A). This observation suggests that the interaction between APPL1 and GIPC1 is not regulated by NGF treatment. In addition to APPL1, TrkA was present in GIPC1 immunoprecipitates from untreated as well as NGF-treated PC12 cells (Fig. 3A). This result, previously reported by Lou et al. (24), is consistent with a model whereby GIPC1 could act to bridge an interaction between APPL1 and TrkA.

The PTB domain of APPL1 interacts directly with TrkA in a phosphotyrosine-independent manner. In addition to the link between APPL1 and TrkA through GIPC1, APPL1 could couple to TrkA through the PTB domain of APPL1 itself. Key signaling molecules downstream of TrkA, including Shc and FRS2, are recruited via their PTB domains to the tyrosine 490 docking site on TrkA, connecting TrkA to the Ras pathway. The binding profile of the PTB domain of APPL1 has recently been determined using peptides based on sequences of putative and known PTB domain-binding sites in the proteome spotted on a peptide array. Utilizing this approach, the APPL1 PTB domain was shown to associate directly with peptides corresponding to the Shc-binding site of TrkA and TrkC (M. Smith and T. Pawson, personal communication).

To explore the possibility that the Shc-binding site of TrkA might be involved in an association with APPL1, biotinylated peptides containing a sequence corresponding to the Shc-binding site were bound to streptavidin Sepharose beads and incubated with lysates of PC12 (6-24) cells. As a positive control, the precipitated complex was immunoblotted with antibodies against ShcA. Three isoforms of ShcA associated specifically

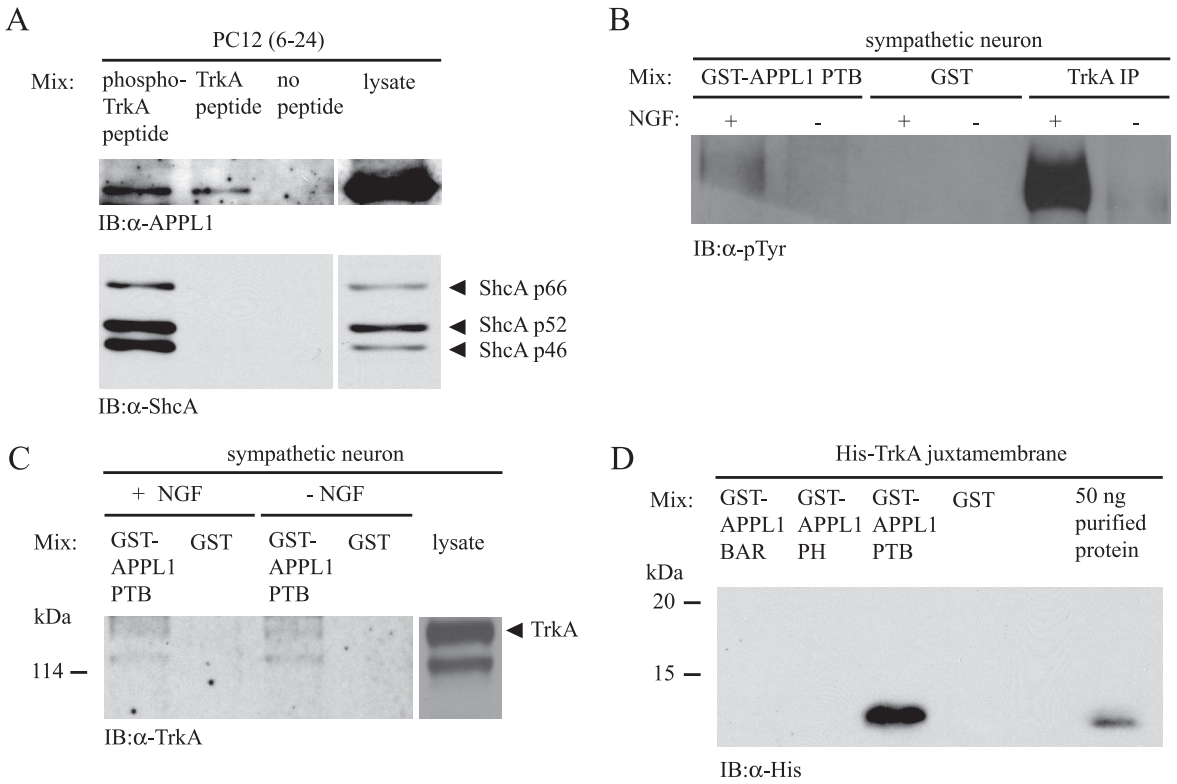

FIG. 5. The PTB domain of APPL1 binds directly to Trk receptors in a phosphotyrosine-independent manner. (A) APPL1 binds to TrkA peptides corresponding to the Shc-binding site. Biotinylated phosphopeptide containing the TrkA sequence PHIIENPQpYFSD or the unphosphorylated version of the peptide was bound to streptavidin beads and incubated with lysates of PC12 (6-24) cells. Streptavidin beads bound only to biotin were included as a negative control. Endogenous APPL1 was detected by immunoblotting (IB) with anti-APPL1 antibodies, and blots were also probed with anti-ShcA antibodies as a positive control. (B) pTrkA associates with the PTB domain of APPL1. NGF was withdrawn from primary cultures of sympathetic neurons, and the cells were treated with 50 ng/ml NGF for 10 min (+) or left untreated (−). Lysates were incubated with GST-APPL1 PTB or GST alone as a negative control or were immunoprecipitated (IP) with a pan-Trk antibody as a positive control. Endogenous pTrkA representing the NGF-activated form of TrkA was detected by immunoblotting with antiphosphotyrosine antibody. (C) The association between the APPL1 PTB domain and TrkA is phosphotyrosine independent. Experiments were performed as described for panel B. Immunoblots were probed with anti-TrkA antibody to detect both phosphorylated and unphosphorylated forms of TrkA. The mature, glycosylated TrkA protein is marked with an arrowhead. The additional lower band in the TrkA immunoblot corresponds to an immature, underglycosylated form of TrkA. (D) The PTB domain of APPL1 interacts directly with the juxtamembrane region of TrkA. A purified His-tagged fragment of TrkA containing the juxtamembrane region was incubated with GST fusions of the APPL1 BAR, PH, and PTB domains or with GST alone. Purified His-TrkA juxtamembrane protein (50 ng) is included as a control. The immunoblot was probed with antibody against the His tag.

with the TrkA peptide phosphorylated at tyrosine 490 but not the unphosphorylated peptide, indicating the efficacy of the peptides in binding their predicted targets (Fig. 5A). Reprobing with antibodies against APPL1 determined that endogenous APPL1 associated with the phosphorylated as well as the unphosphorylated TrkA peptide but not to streptavidin beads bound only to biotin (Fig. 5A). This result indicates that APPL1 can associate with the Shc-binding site of TrkA in a phosphotyrosine-independent manner.

Next, we sought to determine if the PTB domain of APPL1 could mediate its interaction with TrkA. A GST fusion of the APPL1 PTB domain was incubated with lysates of sympathetic neurons that were treated with 50 ng/ml NGF for 10 min or were washed to remove NGF. The GST fusion encompassed only the PTB domain (residues 472 to 655) of APPL1 and did not include the C-terminal PDZ domain-binding site so that the interaction of the PTB domain with TrkA could be assessed independently of GIPC1 (Fig. 2A). We subjected the resulting complexes to Western blotting with an antiphosphotyrosine antibody to detect endogenous pTrkA. pTrkA bound to the GST fusion of the PTB domain of APPL1 but not to GST alone (Fig. 5B). In this experiment, immunoblotting with the antiphosphotyrosine antibody did not allow for the detection of unphosphorylated TrkA. The blots from the GST pull-down experiments were therefore also probed with antibodies against TrkA. This approach revealed that GST-APPL1 PTB interacted with TrkA in the lysate of sympathetic neurons treated with NGF as well as in untreated cells (Fig. 5C). Consistent with the results of the peptide mixing experiment, these data indicate that the APPL1 PTB domain, like the PTB domains found in the X11, Numb, and Fe65 proteins, does not require ligand phosphorylation for binding to its target sequences.

To determine if the interaction between the APPL1 PTB domain and TrkA is direct, purified proteins were employed in binding experiments. His-tagged fusions of the juxtamembrane, kinase, and C-terminal regions of TrkA were added to GST fusions of the APPL1 BAR, PH, and PTB domains immobilized on glutathione Sepharose beads. In mixing experi-

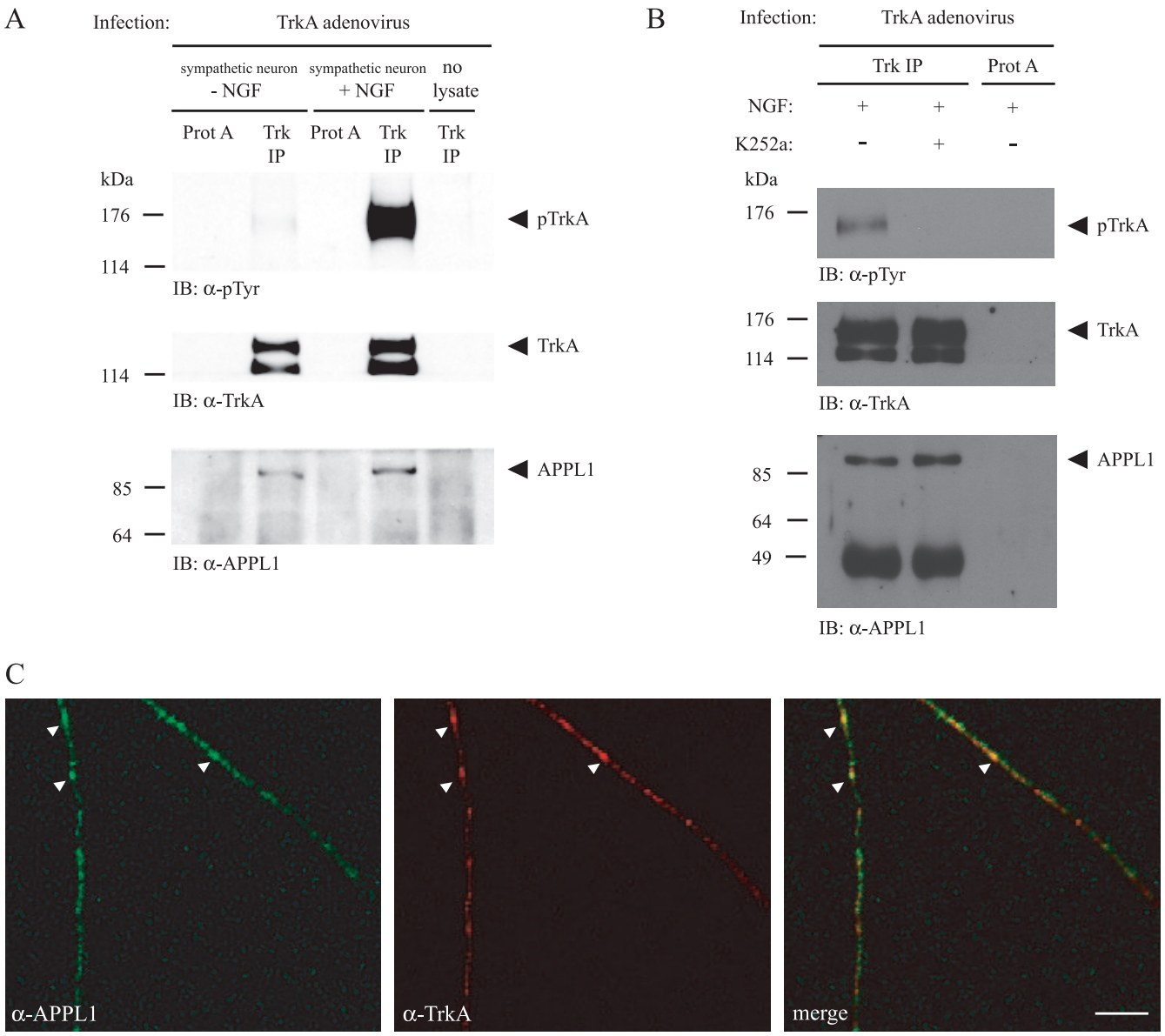

FIG. 6. Endogenous APPL1 coprecipitates with TrkA. (A) Sympathetic neurons infected with Flag-TrkA adenovirus were subjected to NGF withdrawal and then treated with 50 ng/ml NGF for 10 min (+NGF) or left untreated (−NGF). TrkA was immunoprecipitated (IP) from lysates by use of an anti-pan-Trk antibody. Precipitation of lysates with protein A Sepharose (Prot A) alone and the incubation of pan-Trk antibody in the absence of lysate were included as negative controls. Immunoblots (IB) were probed with the indicated antibodies. APPL1, pTrkA, and TrkA bands are marked with arrowheads. The additional band in the TrkA immunoblot corresponds to an immature, underglycosylated form of TrkA. (B) Association of endogenous APPL1 with TrkA does not require TrkA catalytic activity. Experiments were performed as described for panel A, but cells were treated either with 200 nM of the inhibitor K252a in DMSO (+) or with DMSO alone (−). (C) TrkA and APPL1 display partially overlapping distributions in the axons of rat primary sympathetic neurons cultured in medium containing NGF. Confocal images were taken of neurons stained with antibodies against APPL1 (green) or TrkA (red). The rightmost panel shows the merged image. Arrowheads mark examples of the overlap between TrkA and APPL1 distribution. Bar, 5 μm.

ments, only the APPL1 PTB domain exhibited binding to the juxtamembrane region of TrkA that contains the Shc-binding site (Fig. 5D). No binding of the APPL1 PTB domain to the kinase or the C-terminal region of TrkA was detected (data not shown). Taken together, these results clearly show that the PTB domain of APPL1 can bind directly to TrkA in both its tyrosine-phosphorylated and unphosphorylated forms.

Endogenous APPL1 associates with TrkA in sympathetic neurons. Having identified two possible routes through which APPL1 can couple with TrkA, we next evaluated whether APPL1 and TrkA associate in sympathetic neurons. TrkA was immunoprecipitated from a mass culture of neurons infected with adenovirus encoding TrkA to elevate the level of the receptor. Endogenous APPL1 specifically coprecipitated with TrkA from infected neurons (Fig. 6A). The interaction appeared to be independent of TrkA phosphorylation as it was observed both in sympathetic neurons treated with 50 ng/ml NGF for 10 min and in cells washed free of NGF. The speci-

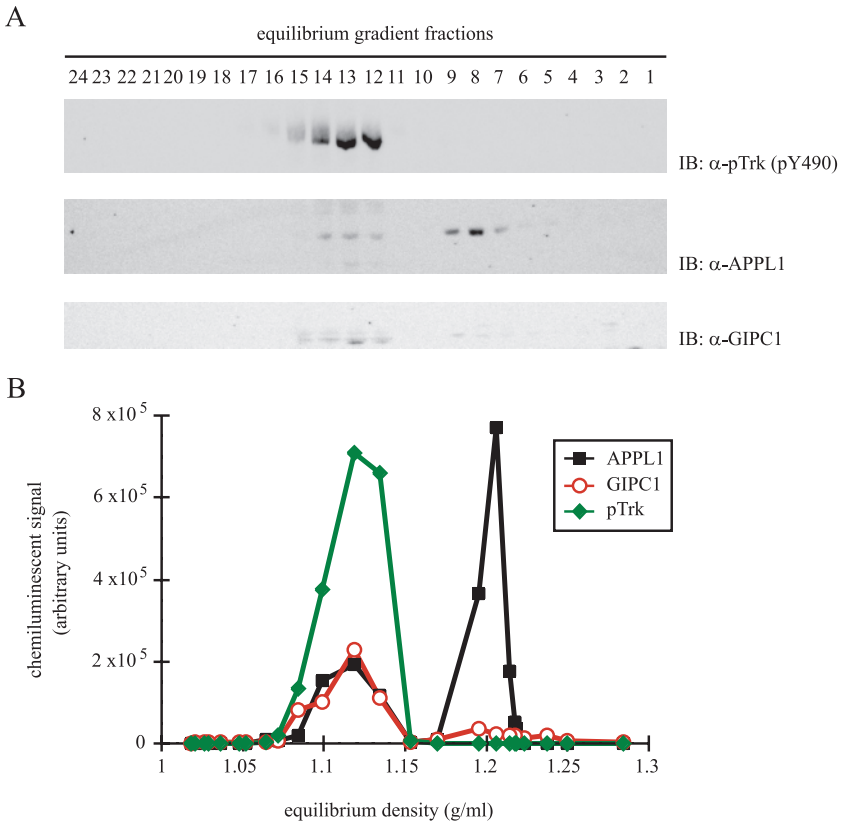

FIG. 7. pTrkA, APPL1, and GIPC1 are present together in endosomal subfractions. (A) Fractions of endosomes from NGF-treated PC12 cells were isolated and then separated on the basis of size by velocity centrifugation. Five velocity gradient fractions were collected, and each pool was further resolved on flotation equilibrium gradients. Data from an equilibrium gradient of velocity gradient fraction 2 are shown. Equilibrium gradient fractions were collected such that endosomes of higher density are contained in lower-numbered fractions. Proteins were resolved by SDS-PAGE, and the immunoblot (IB) was probed with the indicated antibodies. (B) Quantification and graphical representation of the data shown in panel A. The density of each fraction was determined by refractive index measurements. Chemiluminescent signal strength from each of the pTrk, APPL1, and GIPC1 bands was quantified and plotted against density. Data shown in panels A and B are representative of three separate experiments.

ficity of the interaction was confirmed by the absence of APPL1 in samples precipitated with protein A Sepharose alone or with anti-TrkA antibodies in the absence of lysate.

To evaluate if TrkA catalytic activity was required for the interaction with APPL1, similar experiments were performed but in the presence or absence of the Trk inhibitor K252a. Coprecipitation of endogenous APPL1 with TrkA was observed whether the cells were treated with K252a in dimethyl sulfoxide (DMSO) or with DMSO alone, demonstrating that receptor autophosphorylation by the kinase domain of TrkA is not required for the APPL1 interaction (Fig. 6B).

As another approach to examine the association of APPL1 with TrkA in sympathetic neurons, cultured neurons were subjected to immunofluorescence staining to examine the distribution of these proteins. Costaining to detect TrkA and APPL1 determined a partially overlapping pattern of distribution along axonal tracts (Fig. 6C). Taken together, the coimmunoprecipitation and immunofluorescence data indicate that APPL1 and TrkA can associate in sympathetic neurons.

APPL1 and GIPC1 are present with phosphorylated TrkA in endosomal fractions. APPL1 has been reported to localize to endosomes that perform a signaling function downstream of EGF (26). Having demonstrated an association between APPL1 and TrkA, we were interested in determining if these proteins also share a common endosomal distribution. To address this issue, we performed a series of fractionation steps to separate different populations of endosomes at a high resolution on the basis of their physical properties. PC12 cells were treated with NGF for 10 min, a well-characterized time point at which most of the NGF is present with the TrkA receptor in endocytic organelles (10, 11). Endosomes were isolated from permeabilized cells and separated first by their mass using velocity centrifugation. Five velocity gradient fractions were collected, and each of these was subjected to centrifugation through an equilibrium flotation gradient to resolve endocytic organelles by density.

Analysis of equilibrium gradient fractions by SDS-PAGE and immunoblotting with antibodies against pTrkA (anti-pY490), APPL1, and GIPC1 revealed that one population of pTrkA-positive endosomes also contained APPL1 and GIPC1 (Fig. 7A and B). pTrkA, APPL1, and GIPC1 are present together in fractions 12 through 15, and all three proteins have a peak at fraction 13, corresponding to a density of 1.12 g/ml. This result, taken together with the coimmunoprecipitation data, strongly suggests that these proteins associate in endosomes after treatment of PC12 cells with NGF. Interestingly, APPL1 is also present in fractions 6 through 9, with a peak at

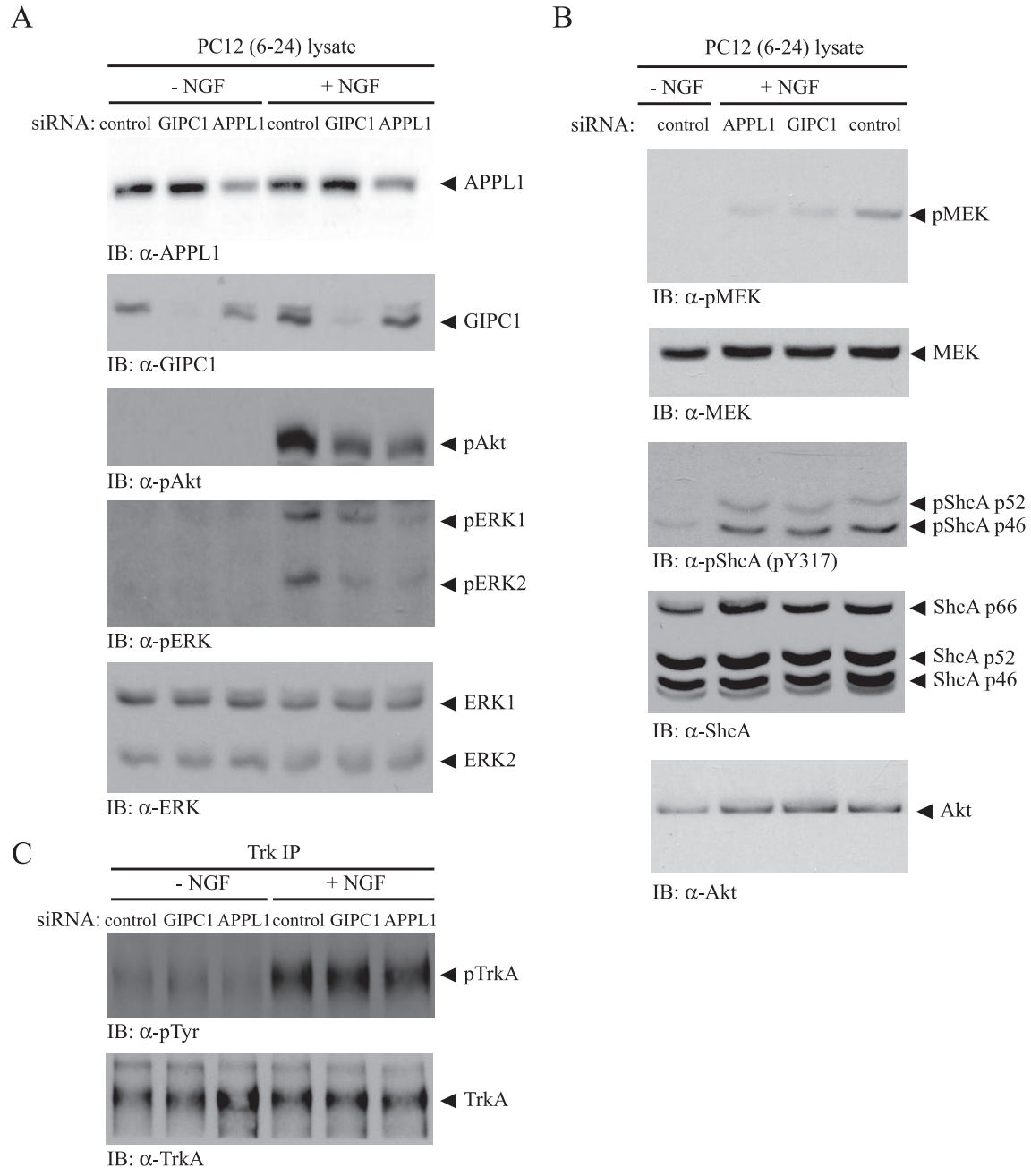

FIG. 8. Reduction of APPL1 and GIPC1 protein levels by RNA interference decreases ERK and Akt activation but does not affect TrkA tyrosine phosphorylation. (A) pERK and pAkt are reduced in APPL1 or GIPC1 siRNA-treated cells. PC12 (6-24) cells were transfected with a negative-control siRNA or siRNAs targeting GIPC1 or APPL1. After NGF withdrawal, cells were treated with 50 ng/ml NGF for 10 min (+NGF) or left untreated (−NGF). Equal amounts of cell extract (30 μg total protein) were analyzed by immunoblotting (IB) with the indicated antibodies. Levels of ERK1 and ERK2 were detected as a control for the specificity of the siRNA treatment. (B) MEK activation is decreased whereas ShcA phosphorylation is unaffected in APPL1 and GIPC1 siRNA-treated cells. The same lysates from the experiments described for panel A were probed with antibodies against pMEK, MEK, pShcA (pY317), ShcA, and Akt. (C) Neither TrkA levels nor levels of TrkA total tyrosine phosphorylation are affected by reduction of APPL1 and GIPC1 protein levels. TrkA was immunoprecipitated (IP) from 100 μg of the lysates from the same experiment shown in panels A and B. Immunoblots were probed with antibodies against TrkA and phosphotyrosine.

1.21 g/ml. In these fractions, pTrkA was not detectable. This observation indicates that there is at least one other population of endosomes bearing APPL1 that is not involved in TrkA trafficking and signaling.

Reduction of APPL1 or GIPC1 levels decreases NGF-induced MEK, ERK, and Akt activation. The interactions of GIPC1 and APPL1 with TrkA suggest that these proteins play a role in receptor function. To examine the functional conse-

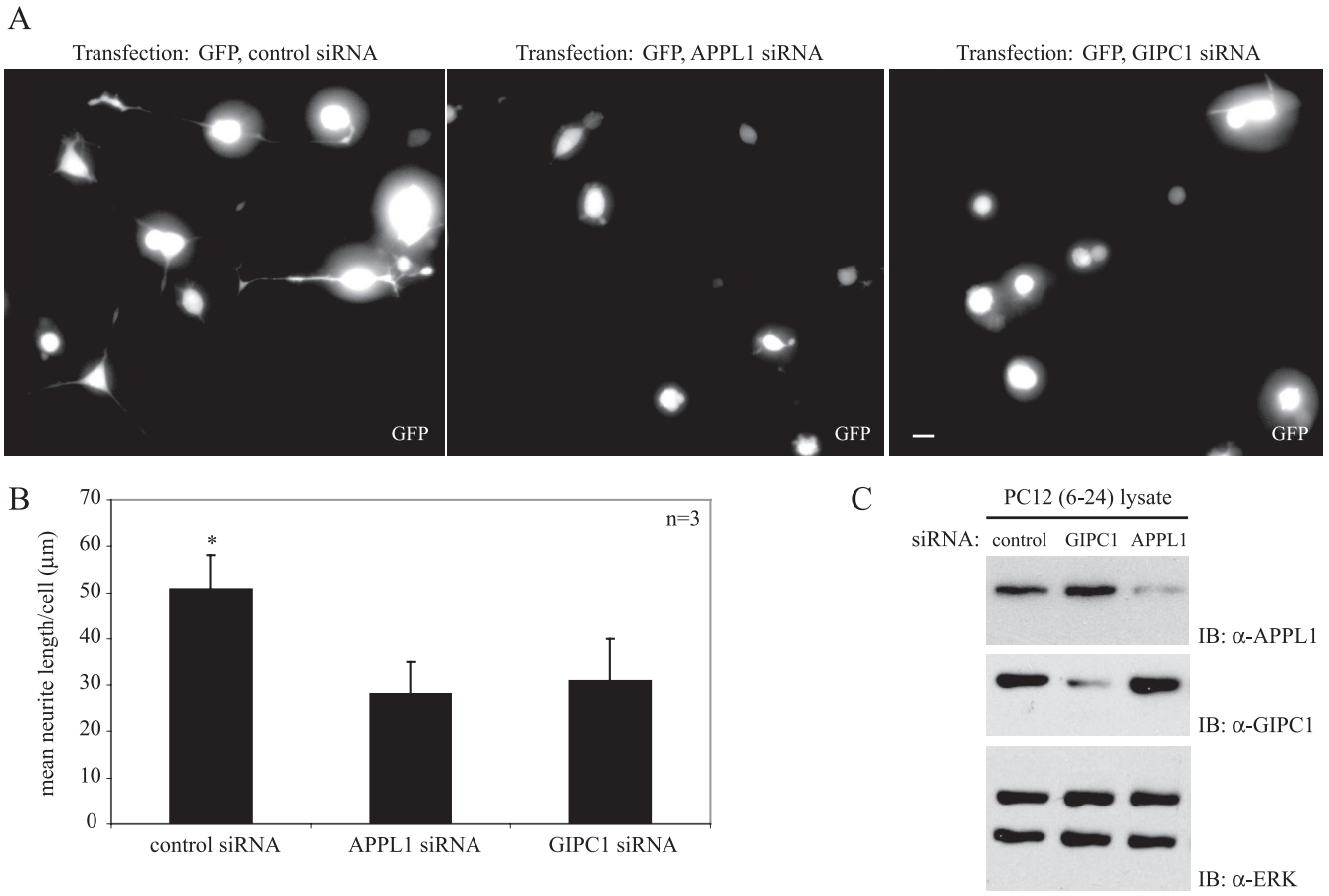

FIG. 9. Reduction of APPL1 or GIPC1 levels decreases NGF-induced neurite outgrowth. (A) GFP epifluorescence in fields of NGF-differentiated PC12 (6-24) cells following siRNA treatment. Cells were cotransfected with the indicated siRNA and with pEGFP to allow for visualization of neurites. Twenty-four hours following transfection, cells were differentiated by treatment with 50 ng/ml NGF for 48 h. Bar, 10 μm. (B) Effect of RNA interference-mediated reduction of APPL1 or GIPC1 levels on neurite outgrowth in PC12 (6-24) cells. Neurite lengths were measured 48 h following NGF treatment, 72 h posttransfection. Mean neurite lengths per cell from three independent experiments ($n = 3$) are shown, along with standard errors. Cells treated with siRNAs targeting APPL1 or GIPC1 have significantly shorter average neurite lengths than those transfected with the control siRNA ($P < 0.02$, Bonferroni and Tukey tests on a paired design). (C) Levels of APPL1 and GIPC1 protein are reduced in the cells shown in panel A. Following immunofluorescence analysis, cells were lysed and levels of APPL1 and GIPC1 were analyzed by immunoblotting (IB) with the indicated antibodies. ERK levels provided a control for equal loading.

quences of reducing APPL1 or GIPC1 protein levels on TrkA signaling, PC12 (6-24) cells were transfected with synthetic siRNAs targeting either APPL1 or GIPC1 or with a control siRNA of random sequence. After 48 h, serum-starved cells were treated with 50 ng/ml NGF for 10 min. Transfection of PC12 (6-24) cells with siRNAs directed against GIPC1 or APPL1 effectively and specifically reduced endogenous levels of these proteins (Fig. 8A). Densitometric analysis of the blots shown in Fig. 8A indicated an approximate reduction of GIPC1 protein levels to 8% and 15% of the level observed for cells treated with the control siRNA in the absence or presence of NGF, respectively, upon GIPC1 siRNA treatment. APPL1 protein was detected at 39% and 48% of control levels for the conditions without or with NGF, respectively, upon APPL1 siRNA treatment. The siRNA-mediated decrease of APPL1 did not affect GIPC1 levels, nor did reduction of GIPC1 affect APPL1 levels. As expected, transfection of the control siRNA had no effect on either APPL1 or GIPC1 levels. ERK1 and ERK2 levels were unaffected in treated cells, confirming the targeting specificity of the siRNAs.

NGF-induced signaling downstream of the TrkA receptor was assayed by measuring levels of ERK, MEK, and Akt activation. In cells treated with either GIPC1 or APPL1 siRNAs, NGF-induced ERK1 and ERK2 phosphorylation was significantly diminished in comparison to cells treated with the control siRNA (Fig. 8A). Densitometric analysis revealed that levels of NGF-mediated phosphorylation of ERK1 and ERK2 were reduced to 22% and 21% of control levels, respectively, in APPL1 siRNA-treated cells. A decrease to 63% for pERK1 and 32% for pERK2 was observed for cells treated with GIPC1 siRNA. A similar pattern of reduction was observed when NGF-stimulated MEK phosphorylation was evaluated (Fig. 8B). pMEK levels were decreased in APPL1 siRNA-treated cells to 29% of control siRNA levels and GIPC1 siRNA-treated cells to 41% of control siRNA levels. Examination of phospho-Akt levels determined that NGF-induced Akt activa-

tion was also reduced in PC12 (6-24) cells transfected with APPL1 siRNA to 39% of control siRNA levels or with GIPC1 siRNA to 61% of control siRNA levels (Fig. 8A). In addition, we examined the tyrosine phosphorylation of ShcA and FRS2, two proximal targets of TrkA known to regulate MEK and MAPK activity. We did not detect a reduction in the tyrosine phosphorylation of ShcA (Fig. 8B) or FRS2 (data not shown) in cells treated with APPL1 or GIPC1 siRNA. These results indicate that APPL1 and GIPC1 are involved in activation of the MAPK pathway as well as the PI 3-kinase/Akt pathway downstream of TrkA and ShcA but upstream of MEK.

One possible explanation for the reduction in both pERK and pAkt levels is that NGF-induced TrkA activation may be compromised as a result of reduced APPL1 or GIPC1 levels. To test this possibility, we immunoprecipitated TrkA from lysates of the same experiment described above and examined its level of phosphorylation by use of an antiphosphotyrosine antibody. In contrast to the effects on ERK and Akt activation, TrkA total phosphorylation was not affected by the down-regulation of endogenous APPL1 or GIPC1 (Fig. 8C). These data demonstrate that GIPC1 and APPL1 function in NGF-induced ERK and Akt phosphorylation downstream of TrkA activation.

Neurite outgrowth is diminished in cells with decreased APPL1 or GIPC1 levels. Having determined a requirement for APPL1 and GIPC1 in NGF-induced ERK and Akt activation, we next investigated whether these proteins were necessary for biological outcomes mediated by NGF signaling. We explored this possibility by using PC12 cells as a model to examine the role of GIPC1 and APPL1 in NGF-induced neurite extension. PC12 (6-24) cells plated on poly-L-lysine to assist in their differentiation were cotransfected with pEGFP and siRNA oligonucleotides. After 24 h, cells were differentiated for 2 days in media containing 50 ng/ml NGF. Expression of GFP was used to visualize neurites in transfected cells. The ratio of pEGFP DNA to siRNA oligonucleotide was optimized so that the majority of GFP-positive cells were cotransfected with the siRNA (data not shown).

Examination of neurite length revealed that, in comparison to cells treated with the control siRNA, cells extended short processes when APPL1 or GIPC1 levels were reduced by siRNA treatment (Fig. 9A). We quantified this effect by measuring the neurite lengths of GFP-positive cells. Compared with an average length of 50.7 ± 7.4 μm per cell for the control siRNA-treated cells, cells treated with APPL1 siRNA and GIPC1 siRNA had an average neurite length of 28.2 ± 6.8 μm per cell and 30.8 ± 9.2 μm per cell, respectively (Fig. 9B). Thus, reduced levels of APPL1 or GIPC1 significantly attenuated NGF-induced neurite outgrowth relative to that for control-treated cells ($P < 0.02$). This effect on growth is consistent with the observed decrease in NGF-mediated activation of the ERK pathway. Following the capture of images by immunofluorescence microscopy, the cells were lysed and proteins levels examined by immunoblotting with antibodies against GIPC1, APPL1, and ERK. APPL1 and GIPC1 protein levels were reduced upon treatment with their respective siRNAs, while ERK levels were unaffected, confirming the effective knockdown of endogenous APPL1 or GIPC1 protein levels in these cells (Fig. 9C).

Since we observed a reduction in the activation of the Akt pathway as a result of knockdown of APPL1 or GIPC1 protein levels, we assayed for effects on cell survival. We performed Hoechst staining on the siRNA-treated, NGF-differentiated PC12 (6-24) cells. Analysis revealed that $3.2\% \pm 0.9\%$ of control siRNA-treated, $7.6\% \pm 1.7\%$ of GIPC1 siRNA-treated, and $6.2\% \pm 0.8\%$ of APPL1 siRNA-treated cells displayed condensed or fragmented nuclei, indicative of apoptosis. To further verify that the siRNA-treated cells were not simply undergoing widespread cell death, survival was quantified by an MTT assay that measures mitochondrial function. When standardized to a value of 100% for the control siRNA-treated cells, MTT readings for GIPC1 siRNA-treated cells were an average of $92.5\% \pm 3\%$ ($n = 3$) and readings for APPL1 siRNA-treated cells were $91.4\% \pm 5.3\%$ ($n = 3$). The limited extent of apoptosis as assayed by both Hoechst staining and MTT assay suggests that the effects of reducing APPL1 or GIPC1 protein levels on neurite length are not a consequence of an impact upon cell survival but rather result from a perturbation of neurite outgrowth mediated by the ERK pathway downstream of the TrkA receptor.

DISCUSSION

In this report, we have identified APPL1 as a novel TrkA-associated protein in neurons. APPL1, which is known to play roles in endosomal signaling and Akt regulation, was also found to be associated with GIPC1, another TrkA-interacting protein previously shown to cluster with TrkA in intracellular vesicles. The association of APPL1 and TrkA could occur by at least two mechanisms, one requiring GIPC1 and the second through the direct binding of the APPL1 PTB domain to TrkA. The binding of APPL1 to GIPC1 was mediated by the C-terminal region of APPL1 and the PDZ domain of GIPC1. APPL1, GIPC1, and activated TrkA cofractionated in the same highly purified endosomal membrane preparation from PC12 cells. Both APPL1 and GIPC1 were required for TrkA signal transduction, as reduction of the levels of either of these proteins suppressed NGF-stimulated ERK1/2 and Akt activation and neurite outgrowth in PC12 cells.

What is the function of APPL1 in NGF-mediated signal transduction? We found that the suppression of APPL1 levels inhibited NGF-mediated Akt and Erk activation, which are required for NGF-mediated survival and neuritogenesis, respectively (19). APPL1 has been reported to be a direct binding partner for Akt2 and postulated to potentiate Akt activation by tethering this kinase to PI 3-kinase (27). Consistent with this hypothesis, APPL1 enhanced Akt-mediated suppression of androgen receptor transactivation in a PI 3-kinase-dependent manner and was required for Akt phosphorylation on serine residue 473 in response to insulin-like growth factor in PC-3 cells (38). A similar role for APPL1 is suggested by our observation that reducing APPL1 levels decreased NGF-mediated Akt phosphorylation. The reduction of Akt activity by suppression of APPL1 levels, however, did not suppress NGF-induced PC12 cell survival, likely because the residual levels of Akt were sufficient to mediate survival. In support of this conclusion, sympathetic neurons are known to require 10-fold less NGF for survival than for axonal growth (3).

Our experiments also revealed a requirement for APPL1 in NGF-induced activation of MEK and ERK1/2 but not TrkA

activation or ShcA phosphorylation. In PC12 cells and sympathetic neurons, activation of the MAPK pathway is required for NGF-mediated neuritogenesis (19). Consistent with this role of the MAPK pathway downstream of NGF, we demonstrated that the suppression of APPL1 levels also attenuated NGF-induced neuritogenesis. Interestingly, APPL1 was previously shown to weakly associate with Grb2 (27), an adaptor protein that regulates TrkA-induced MAPK activity, providing a possible means by which APPL1 regulates the activity of this pathway.

The observation that APPL1 associates with TrkA and cofractionates with TrkA in a subpopulation of endosomes is consistent with a model whereby APPL1 may function in endosomal signaling downstream of NGF. APPL proteins have previously been implicated in an EGF-induced endosomal signaling pathway that links trafficking events at the plasma membrane to chromatin remodeling in the nucleus (26). In EGF-treated HeLa cells, APPL was required for EGF-induced cell proliferation through uptake of EGF into APPL- and Rab5-containing endosomes at membranes and transport and release of APPL to the nuclear compartment. While we have thus far not observed an NGF-mediated translocation of APPL1, the association between these proteins may serve to couple NGF-TrkA endosomal signaling complexes to other trafficking events governed by the Rab proteins. This hypothesis is consistent with the emerging theme that Rab GTPases are significant players in TrkA trafficking and signaling. Indeed, Rab7 was recently identified to associate with TrkA to regulate the signaling endosome residence time (29) and Rab5 has been found with GIPC1, APPL1, and pTrkA in endosomal fractions of NGF-treated PC12 cells (M. Grimes, personal communication).

We found that APPL1 associated with GIPC1, a TrkA-binding protein that has previously been shown to be required for activation of NGF-induced MAPK signaling (24). We show that GIPC1 is also required for efficient NGF-induced neurite outgrowth, as well as activation of MEK, MAPK, and Akt. The precise mechanism through which GIPC1 mediates these functions remains to be elucidated. However, the observed effects of reducing GIPC1 levels are similar to those of decreasing APPL1 levels. Furthermore, we have identified a direct PDZ domain-mediated association between GIPC1 and APPL1 and have detected APPL1, GIPC1, and phosphorylated TrkA in the same endosomal fractions. Based on these observations, we propose that GIPC1 may function as a bridging protein to connect APPL1 with TrkA. Despite containing only a single protein-protein interaction domain, GIPC1 has been hypothesized to function as a scaffolding molecule to organize multiprotein complexes. Interestingly, mutation of the carboxylate binding loop of the GIPC1 PDZ domain does not abolish the interaction between TrkA and GIPC1, raising the possibility that the binding pocket of the GIPC1 PDZ domain remains open to recruit other proteins (24). Therefore, it is conceivable that GIPC1 can simultaneously engage both TrkA and APPL1 since the binding of the internal sequence in the juxtamembrane region of TrkA occurs at a site within the GIPC1 PDZ domain that is distinct from the carboxylate binding pocket that interacts with the C-terminal sequence of APPL1. Another mechanism by which GIPC1 can organize higher-order complexes containing both APPL1 and TrkA is through the ability of GIPC1 to multimerize, a process involving its N-terminal domain (5). This versatility in protein interactions allows GIPC1 to bridge distinct pathways by simultaneously binding different proteins. For example, GIPC1 can recruit GAIP, a regulator of heterotrimeric G proteins, to TrkA (24) and to the D_2R dopamine receptor (17). We suggest that GIPC1 may play an important role in TrkA function by bridging the association between APPL1 and TrkA.

The APPL1 PTB domain bound TrkA directly without the involvement of GIPC1. The availability of both GIPC1-dependent and GIPC1-independent routes for APPL1 association with TrkA suggests that the composition of the internalized TrkA signaling complex may be dynamic. One possibility is that the GIPC-dependent association may be important in early events after TrkA activation while the GIPC1-independent interaction comes into play during later events. Several lines of evidence suggest GIPC1 is involved in endocytosis and early trafficking events after receptor internalization. In nonneuronal cells, GIPC1 localizes to membrane-associated vesicles and tubular structures and to clathrin-coated pits (23). We have shown the presence of GIPC1, APPL1, and activated TrkA in endosomal fractions 10 min after NGF treatment. This observation is in agreement with fractionation studies with PC12 cells and cortical neurons showing similar profiles of enrichment within fractions of intracellular membranes for GIPC1 and Trk (39). During the course of TrkA endocytosis and trafficking, however, GIPC1 or APPL1 may not remain associated with TrkA. The dissociation of GIPC1 from vesicles after fusion with early endosomes in epithelial cells (1) and nonexhaustive colabeling of GIPC1 with D_2R and D_3R dopamine receptors (16) suggest that GIPC1 is released during later sorting events. At these later time points, GIPC1-independent binding via the APPL1 PTB domain may be the mechanism through which TrkA and APPL1 continue to associate in neuronal cells.

Based upon our observations, we propose a model whereby APPL1 and GIPC1 are constitutively bound to TrkA. Upon activation of TrkA by NGF, APPL1 potentiates Akt activation at the plasma membrane. Both GIPC1 and APPL1 are cointernalized with activated TrkA, residing in a population of endosomes that target TrkA to signaling proteins, such as MAPK, or to the nuclear membrane. Future experiments assessing the effect of disrupting APPL1, GIPC, and TrkA interactions in primary neurons in compartmentalized cultures will allow us to further elucidate the role of these proteins in the transmission of NGF retrograde signals.

ACKNOWLEDGMENTS

We thank M. Chao and Jerry Gish for generously supplying the GIPC1 antibodies and TrkA peptides, respectively. We are grateful to B. M. Kramer and F. Robinson for critical reading of the manuscript and to J. F. Lavoie for assistance in the statistical analysis of the data.

This work was supported by a Canadian Institutes of Health Research (CIHR) postdoctoral fellowship to D.C.L., a postdoctoral fellowship from the Ministry of Education and Science of Spain to C.Q., an NIH grant (RO1 CA 77429) to J.R.T., proteomic grants to John Bergeron, McGill University, from the CFI, CIHR, Genome Quebec, Genome Canada, and Valorisation Recherche de Quebec, and a CIHR operating grant to D.R.K. and F.D.M. F.D.M. and D.R.K. are recipients of Canada Research Chairs.

REFERENCES

1. **Aschenbrenner, L., T. T. Lee, and T. Hasson.** 2003. Myo6 facilitates the translocation of endocytic vesicles from cell peripheries. Mol. Biol. Cell **14:**2728–2743.
2. **Beattie, E. C., J. Zhou, M. Grimes, N. Bunnett, C. L. Howe, and W. C. Mobley.** 1996. A signaling endosome hypothesis to explain NGF actions: potential implications for neurodegeneration. Cold Spring Harbor Symp. Quant. Biol. **61:**389–406.
3. **Belliveau, D. J., I. Krivko, J. Kohn, C. Lachance, C. Pozniak, D. Rusakov, D. Kaplan, and F. D. Miller.** 1997. NGF and neurotrophin-3 both activate TrkA on sympathetic neurons but differentially regulate survival and neuritogenesis. J. Cell Biol. **136:**375–388.
4. **Bhattacharyya, A., F. L. Watson, T. A. Bradlee, S. L. Pomeroy, C. D. Stiles, and R. A. Segal.** 1997. Trk receptors function as rapid retrograde signal carriers in the adult nervous system. J. Neurosci. **17:**7007–7016.
5. **Bunn, R. C., M. A. Jensen, and B. C. Reed.** 1999. Protein interactions with the glucose transporter binding protein GLUT1CBP that provide a link between GLUT1 and the cytoskeleton. Mol. Biol. Cell **10:**819–832.
6. **Delcroix, J. D., J. S. Valletta, C. Wu, S. J. Hunt, A. S. Kowal, and W. C. Mobley.** 2003. NGF signaling in sensory neurons: evidence that early endosomes carry NGF retrograde signals. Neuron **39:**69–84.
7. **Ehlers, M. D., D. R. Kaplan, D. L. Price, and V. E. Koliatsos.** 1995. NGF-stimulated retrograde transport of trkA in the mammalian nervous system. J. Cell Biol. **130:**149–156.
8. **Engqvist-Goldstein, A. E., M. M. Kessels, V. S. Chopra, M. R. Hayden, and D. G. Drubin.** 1999. An actin-binding protein of the Sla2/Huntingtin interacting protein 1 family is a novel component of clathrin-coated pits and vesicles. J. Cell Biol. **147:**1503–1518.
9. **Ginty, D. D., and R. A. Segal.** 2002. Retrograde neurotrophin signaling: Trk-ing along the axon. Curr. Opin. Neurobiol. **12:**268–274.
10. **Grimes, M. L., E. Beattie, and W. C. Mobley.** 1997. A signaling organelle containing the nerve growth factor-activated receptor tyrosine kinase, TrkA. Proc. Natl. Acad. Sci. USA **94:**9909–9914.
11. **Grimes, M. L., J. Zhou, E. C. Beattie, E. C. Yuen, D. E. Hall, J. S. Valletta, K. S. Topp, J. H. LaVail, N. W. Bunnett, and W. C. Mobley.** 1996. Endocytosis of activated TrkA: evidence that nerve growth factor induces formation of signaling endosomes. J. Neurosci. **16:**7950–7964.
12. **Hempstead, B. L., S. J. Rabin, L. Kaplan, S. Reid, L. F. Parada, and D. R. Kaplan.** 1992. Overexpression of the trk tyrosine kinase rapidly accelerates nerve growth factor-induced differentiation. Neuron **9:**883–896.
13. **Henkemeyer, M., L. E. Marengere, J. McGlade, J. P. Olivier, R. A. Conlon, D. P. Holmyard, K. Letwin, and T. Pawson.** 1994. Immunolocalization of the Nuk receptor tyrosine kinase suggests roles in segmental patterning of the brain and axonogenesis. Oncogene **9:**1001–1014.
14. **Howe, C. L., J. S. Valletta, A. S. Rusnak, and W. C. Mobley.** 2001. NGF signaling from clathrin-coated vesicles: evidence that signaling endosomes serve as a platform for the Ras-MAPK pathway. Neuron **32:**801–814.
15. **Howe, C. L., and W. C. Mobley.** 2004. Signaling endosome hypothesis: a cellular mechanism for long distance communication. J. Neurobiol. **58:**207–216.
16. **Jeanneteau, F., J. Diaz, P. Sokoloff, and N. Griffon.** 2004. Interactions of GIPC with dopamine D_2, D_3 but not D_4 receptors define a novel mode of regulation of G protein-coupled receptors. Mol. Biol. Cell **15:**696–705.
17. **Jeanneteau, F., O. Guillin, J. Diaz, N. Griffon, and P. Sokoloff.** 2004. GIPC recruits GAIP (RGS19) to attenuate dopamine D_2 receptor signaling. Mol. Biol. Cell **15:**4926–4937.
18. **Johanson, S. O., M. F. Crouch, and I. A. Hendry.** 1995. Retrograde axonal transport of signal transduction proteins in rat sciatic nerve. Brain Res. **690:**55–63.
19. **Kaplan, D. R., and F. D. Miller.** 2000. Neurotrophin signal transduction in the nervous system. Curr. Opin. Neurobiol. **10:**381–391.
20. **Lavoie, J. F., L. Lesauteur, J. Kohn, J. Wong, O. Furtoss, C. J. Thiele, F. D. Miller, and D. R. Kaplan.** 2005. TrkA induces apoptosis of neuroblastoma cells and does so via a p53-dependent mechanism. J. Biol. Chem. **280:**29199–29207.
21. **Levi-Montalcini, R.** 1966. The nerve growth factor: its mode of action on sensory and sympathetic nerve cells. Harvey Lect. **60:**217–259.
22. **Levi-Montalcini, R.** 1987. The nerve growth factor 35 years later. Science **237:**1154–1162.
23. **Lou, X., T. McQuistan, R. A. Orlando, and M. G. Farquhar.** 2002. GAIP, GIPC and Gαi3 are concentrated in endocytic compartments of proximal tubule cells: putative role in regulating megalin's function. J. Am. Soc. Nephrol. **13:**918–927.
24. **Lou, X., H. Yano, F. Lee, M. V. Chao, and M. G. Farquhar.** 2001. GIPC and GAIP form a complex with TrkA: a putative link between G protein and receptor tyrosine kinase pathways. Mol. Biol. Cell **12:**615–627.
25. **Mazzoni, I. E., F. A. Said, R. Aloyz, F. D. Miller, and D. Kaplan.** 1999. Ras regulates sympathetic neuron survival by suppressing the p53-mediated cell death pathway. J. Neurosci. **19:**9716–9727.
26. **Miaczynska, M., S. Christoforidis, A. Giner, A. Shevchenko, S. Uttenweiler-Joseph, B. Habermann, M. Wilm, R. G. Parton, and M. Zerial.** 2004. APPL proteins link Rab5 to nuclear signal transduction via an endosomal compartment. Cell **116:**445–456.
27. **Mitsuuchi, Y., S. W. Johnson, G. Sonoda, S. Tanno, E. A. Golemis, and J. R. Testa.** 1999. Identification of a chromosome 3p14.3-21.1 gene, APPL, encoding an adaptor molecule that interacts with the oncoprotein-serine/threonine kinase AKT2. Oncogene **18:**4891–4898.
28. **Patapoutian, A., and L. F. Reichardt.** 2001. Trk receptors: mediators of neurotrophin action. Curr. Opin. Neurobiol. **11:**272–280.
29. **Saxena, S., C. Bucci, J. Weis, and A. Kruttgen.** 2005. The small GTPase Rab7 controls the endosomal trafficking and neuritogenic signaling of the nerve growth factor receptor TrkA. J. Neurosci. **25:**10930–10940.
30. **Shao, Y., W. Akmentin, J. J. Toledo-Aral, J. Rosenbaum, G. Valdez, J. B. Cabot, B. S. Hilbush, and S. Halegoua.** 2002. Pincher, a pinocytic chaperone for nerve growth factor/TrkA signaling endosomes. J. Cell Biol. **157:**679–691.
31. Reference deleted.
32. **Somsel Rodman, J., and A. Wandinger-Ness.** 2000. Rab GTPases coordinate endocytosis. J. Cell Sci. **113:**183–192.
33. **Tsui-Pierchala, B. A., and D. D. Ginty.** 1999. Characterization of an NGF-P-TrkA retrograde-signaling complex and age-dependent regulation of TrkA phosphorylation in sympathetic neurons. J. Neurosci. **19:**8207–8218.
34. **Vaillant, A. R., P. Zanassi, G. S. Walsh, A. Aumont, A. Alonso, and F. D. Miller.** 2002. Signaling mechanisms underlying reversible, activity-dependent dendrite formation. Neuron **34:**985–998.
35. **Valdez, G., W. Akmentin, P. Philippidou, R. Kuruvilla, D. D. Ginty, and S. Halegoua.** 2005. Pincher-mediated macroendocytosis underlies retrograde signaling by neurotrophin receptors. J. Neurosci. **25:**5236–5247.
36. **Wartiovaara, K., F. Barnabe-Heider, F. D. Miller, and D. R. Kaplan.** 2002. N-myc promotes survival and induces S-phase entry of postmitotic sympathetic neurons. J. Neurosci. **22:**815–824.

36a. **Wasiak, S., V. Legendre-Guillemin, R. Puertollano, F. Blondcau, M. Girard, E. de Heuvel, D. Boismenu, A. W. Bell, J. S. Bonifacino, and P. S. McPherson.** 2002. Enthoprotin: a novel clathrin-associated protein identified through subcellular proteomics. J. Cell Biol. **158:**855–862.

37. **Watson, F. L., H. M. Heerssen, D. B. Moheban, M. Z. Lin, C. M. Sauvageot, A. Bhattacharyya, S. L. Pomeroy, and R. A. Segal.** 1999. Rapid nuclear responses to target-derived neurotrophins require retrograde transport of ligand-receptor complex. J. Neurosci. **19:**7889–7900.
38. **Yang, L., H. K. Lin, S. Altuwaijri, S. Xie, L. Wang, and C. Chang.** 2003. APPL suppresses androgen receptor transactivation via potentiating Akt activity. J. Biol. Chem. **278:**16820–16827.
39. **Yano, H., and M. V. Chao.** 2005. Biochemical characterization of intracellular membranes bearing Trk neurotrophin receptors. Neurochem. Res. **30:**767–777.
40. **Ye, H., R. Kuruvilla, L. S. Zweifel, and D. D. Ginty.** 2003. Evidence in support of signaling endosome-based retrograde survival of sympathetic neurons. Neuron **39:**57–68.
41. **Zerial, M., and H. McBride.** 2001. Rab proteins as membrane organizers. Nat. Rev. Mol. Cell Biol. **2:**107–117.